

SCIENTIFIC REPORTS

OPEN

Thermionic Energy Conversion Based on Graphene van der Waals Heterostructures

Shi-Jun Liang¹, Bo Liu², Wei Hu³, Kun Zhou² & L. K. Ang¹

Received: 16 September 2016

Accepted: 10 March 2017

Published: 07 April 2017

Seeking for thermoelectric (TE) materials with high figure of merit (or ZT), which can directly converts low-grade wasted heat (400 to 500 K) into electricity, has been a big challenge. Inspired by the concept of multilayer thermionic devices, we propose and design a solid-state thermionic devices (as a power generator or a refrigerator) in using van der Waals (vdW) heterostructure sandwiched between two graphene electrodes, to achieve high energy conversion efficiency in the temperature range of 400 to 500 K. The vdW heterostructure is composed of suitable multiple layers of transition metal dichalcogenides (TMDs), such as MoS_2 , MoSe_2 , WS_2 and WSe_2 . From our calculations, WSe_2 and MoSe_2 are identified as two ideal TMDs (using the reported experimental material's properties), which can harvest waste heat at 400 K with efficiencies about 7% to 8%. To our best knowledge, this design is the first in combining the advantages of graphene electrodes and TMDs to function as a thermionic-based device.

The most common approach to harvest the waste heat to generate electricity is thermoelectrics (TE), which is based on the Seebeck effect (see Table 1). The performance of TE-based devices is characterized by the figure of merit (ZT), given by ref. 1

$$ZT = \frac{\alpha^2 T}{\frac{\kappa_l}{\mu e} + LT}, \quad (1)$$

where α , T , κ_l , μ , n , and e are, respectively, the Seebeck coefficient, absolute mean temperature, lattice thermal conductivity, carrier mobility, carrier density and electron charge. Here, L is defined as the Lorenz number equal to $2.44 \times 10^{-8} \text{ W } \Omega \text{ K}^{-2}$. This formula has recently been redefined to solve the inconsistency between theoretical prediction and experimental measurement². Before the 1990s, the progress of improving ZT had been slow and the best TE material was Bi_2Te_3 alloys with $ZT \approx 1.0$ at 300 K³. To increase ZT , many new approaches have been proposed^{4,5}, such as fabricating low-dimensional thermoelectric structures to increase large density of state, engineering the interface of materials to reduce the lattice thermal conductivity, and modulating dopants to increase carrier mobility. Subsequently, further improvements include $ZT = 2.4$ at 300 K for p -type $\text{Bi}_2\text{Te}_3/\text{Sb}_2\text{Te}_3$ superlattice⁶, and $ZT = 3$ at 550 K for Bi-doped n -type $\text{PbSeTe}/\text{PbTe}$ quantum-dot superlattice⁷. A prospective of nanostructured TE materials can be found in a review paper⁸. For practical applications, other issue such as size, maintenance and fast response time must also be considered even if high-efficiency TE materials are found ref. 1.

Recent interests in using two-dimensional (2D) transition metal dichalcogenides (TMDs) as new TE materials have attracted extensive attention^{9,10} due to high Seebeck coefficient offered by these 2D TMDs: a bilayer MoS_2 gives $\alpha^2 \sigma = 8.5 \text{ mW/m/K}^2$ ⁹. If this MoS_2 -based TE material is able to realize the calculated thermal conductivity of $\kappa \approx 1.55 \text{ W/m/K}$ ¹¹, we will have $ZT = 1.6$, which corresponds to an efficiency of about 6.5% in harvesting waste heat at T_h (hot side) = 400 K and T_c (cold side) = 300 K [according to Eq. (1)].

For high temperature range, the more viable approach is based on thermionic energy convertor (TIC), which was first proposed by G. N. Hatsopoulos¹². Due to the high work function of the metallic electrode, however TIC is limited to high-temperature operation above 1500 K. A potential method to harvest waste energy at 900 K was

¹SUTD-MIT International Design Center (IDC), Singapore University of Technology and Design (SUTD), 8 Somapah road, 487372, Singapore. ²School of Mechanical and Aerospace Engineering, Nanyang Technological University, 50 Nanyang Avenue, 639798, Singapore. ³Computational Research Division, Lawrence Berkeley National Laboratory, Berkeley, CA 94720, USA. Correspondence and requests for materials should be addressed to L.K.A. (email: ricky_ang@sutd.edu.sg) or S.J.L. (email: shijun_liang@mymail.sutd.edu.sg)

System	d [nm]	κ for [W/m/K]	Experiment SBH [V]	T_R [K]	Optimal SBH [V]	Max η_g [%]
G/MoS ₂	50	0.3	0 to 0.11	847	0	3.15
G/WS ₂	50	0.2125	0 to 0.37	758	0	3.93
G/MoSe ₂	70	0.089	0 to 0.4	501	0.005	7.28
G/WSe ₂	62	0.048	0 to 0.44	428	0.02	8.56

Table 1. The designed parameters: T_R , optimal effective barrier height ϕ' and the calculated efficiency η_g of the proposed power generator operating at $T_h = 400$ K and $T_c = 300$ K based on the experimentally-measured cross-plane thermal conductivity of different TMDs materials at the temperature of 300 K [See S2: Supplementary materials]: (a) 50-nm of Gr/MoS₂/Gr²⁸, (b) 50-nm of Gr/WS₂/Gr²⁸, (c) 70-nm of Gr/MoSe₂/Gr^{27,39} and (d) 62-nm of Gr/WSe₂/Gr^{27,39}.

recently proposed by using a suspended monolayer graphene as cathode to provide an efficiency of higher than 40%¹³. This improvement is attributed to the new thermionic law given by $J(\phi, T, E_F) = A^* \times T^3 \times \exp[-(e\phi - E_F)/k_B T]$, where $A^* = ek_B^3/\pi\hbar^3 v_f^2 = 0.01158 \text{ A/cm}^2/\text{K}^3$, v_f is the Fermi velocity, E_F is the Fermi level, and ϕ is the barrier height at zero bias. Note that the new scaling has been compared well with a recent experiment¹⁴. For the wasted heat generated in the industrial or domestic process, low-grade heat (around 400 K to 500 K) is distributed more everywhere. developing an efficient approach remains a great challenge so far.

In this paper, we propose a high-efficiency solid-state thermionic device by using van der Waals (vdW) heterostructure¹⁵ composed of 2D TMDs (MoS₂, MoSe₂, WS₂, and WSe₂) and graphene electrodes. By taking the advantage of the ultralow cross-plane thermal conductance of the 2D materials and the new thermionic emission over the Schottky barrier (SB) contact between the graphene and 2D materials (tunable via gate voltage or chemical doping), we predict that it is possible to realize high-efficiency power generation and refrigeration at the temperature of 300 K to 500 K, which may be better than (or at least comparable to) the traditional TE devices. Note that the concept of using multi-layers or superlattices in the thermionic devices was first suggested by two groups (Shakouri and Mahan) in late 1990s^{16,17}. The performance of their proposed single-junction thermionic device was predicted to be better than the TE device using the same InGaAs/InAlAs material¹⁸. For simplicity, we will ignore the effect of non-conservation of lateral momentum in the thermionic emission^{18,19} in this paper. This is justified by the facts that Schottky barrier height is planar and homogenous at the interface between graphene and Transition metal dichalcogenide²⁰.

With the current advances in growing graphene and TMDs, the proposed vdW heterostructures such as Gr/TMDs/Gr (Gr is the monolayer graphene) can be assembled experimentally^{15,21–26}. For different 2D TMDs (MoS₂, MoSe₂, WS₂ and WSe₂), the cross-plane thermal conductivity κ was measured to be very low: $\kappa = 0.05 \text{ W/m/K}$ for disordered WSe₂²⁷, $\kappa = 0.0084$ to 0.3 W/m/K for MoS₂, WS₂ and WSe₂²⁸, and $\kappa = 0.085 \text{ W/m/K}$ for 10 nm-thickness of WSe₂ synthesized via Se-O exchange²⁹. Due to their low cross-plane thermal conductivity, these 2D materials may seem to be good TE materials, but having very low electrical mobility³⁰ will also offset the increment due to low thermal conductivity. Thus the thermionic emission-based (or TIC) method may be a better approach than TE method, if the ballistic transport³¹ within the structure can be ensured by choosing a suitable thickness (to avoid collisions) and an optimal barrier height (to have high-current injection). Note that this ballistic assumption is very commonplace in the previous studies of thermionic emission based on the traditional Superlattices structure^{17,18,32}. In the conventional superlattices, the thickness is usually larger than $1 \mu\text{m}$. Compared with the conventional superlattices structure, the van der waals heterostructure made of graphene and TMDs considered in our paper is far less than $1 \mu\text{m}$ in thickness of cross-plane direction. Therefore the ballistic assumption in the cross-plane is justified. Note that Gr/h-BN/Gr heterostructures device³³ has been fabricated to study the thermoelectric transport properties, but the measured low ZT calls for further effort to identify the most ideal sandwiched material and optimized parameters of devices to achieve the goal of high-efficiency thermal energy conversion. In our work presented here, we theoretically identify two materials WSe₂ and MoSe₂, together with employing Molecular dynamics simulations and ab initio calculations. we hope that these two identified candidates materials can further motivate experimentalist to explore the feasibility of achieving high-efficiency thermal energy harvesting system based on thermionic emission mechanism in using other 2D materials assembled in a vdW heterostructure.

Figure 1 illustrates the proposed vdW heterostructure-based thermionic device with two monolayers graphene as top and bottom layers, and N -layers of 2D TMDs materials of thickness d between two graphene layers. This configuration is similar to the recently-reported Gr/phosphorene/Gr³⁴ and Gr/h-BN/Gr sandwich structure³³. The device can be either a power generator or refrigerator depending on the direction of the current flow. For power generation, electron flow is from the hot electrode at temperature T_h to the cold electrode at temperature T_c .

If a 2D material with suitable thickness d and low cross-plane thermal conductivity κ is used as the vdW heterostructure, our calculations show that TIC device may offer higher efficiency as compared to the existing TE devices operating at low-grade temperature (400 to 500 K). As a power generator, it can harvest waste heat at 400 K with about 8% efficiency using the reported experimental properties of the 2D materials.

For refrigeration at 260 K, the efficiency can be more than 40% of the Carnot efficiency. According to our model, the thickness of the layer must be in the intermediate range in order to reach high efficiency. For few layers, electron tunneling process will be dominant over the over-barrier thermionic emission which will reduce the efficiency³⁵. For larger values of d , it will induce a large cross-plane thermal conductivity κ ; and also makes the assumption of ballistic electron transport within the layers no longer valid.

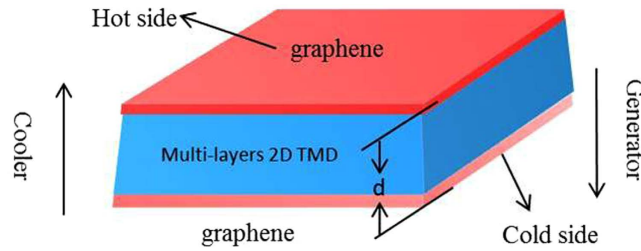


Figure 1. A novel design of solid-state vdW heterostructure-based thermionic devices. This structure is composed of multilayers of 2D TMDs material (such as MoS₂, WS₂, MoSe₂ and WSe₂) with thickness *d* sandwiched between two graphene electrodes. The top graphene electrode is attached to a heat source at temperature *T_h* and the bottom one is maintained at room temperature (*T_c* = 300 K) when functioning as a power generator. The electrons (or holes) are thermally-excited and ballistically transported over the Schottky barrier formed at the interface between the graphene electrodes and 2D vdW structure. As a refrigerator, the cold side is reduced to *T_c* = 260 K through removing the high-energy electrons or holes in the graphene electrode and the heat is carried by the hot electrons (holes) to the hot electrode biased at room temperature *T_h* = 300 K.

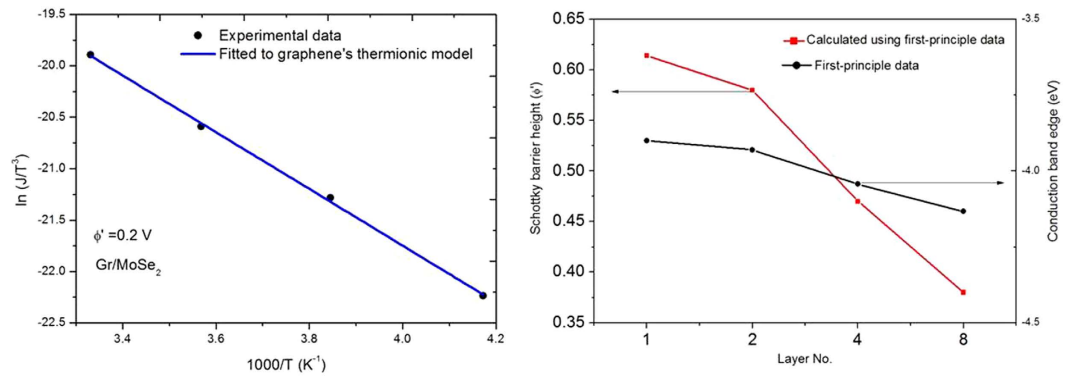


Figure 2. (a) The comparison of the thermionic current for a Gr/MoSe₂ contact between the calculation and experiment results²⁴: $\ln(J/T^3)$ as a function of $1000/T$ with an effective barrier height of $\phi' = 0.2$ V for 44 layers of MoSe₂. **(b)** Schottky barrier height (ϕ') [left y-axis] of graphene/MoSe₂ contact decreases with increasing layer number of MoSe₂, which is calculated³⁷ based on the conduction band edge of MoSe₂ [right y-axis].

For a given voltage of *V*, the electrical current density (*J_e*) and the thermal current density (*J_Q*) being transported across the electrodes are, respectively,

$$J_e = J_c - J_h e^{-\frac{eV}{k_B T_h}}, \tag{2}$$

$$J_Q = \left(\phi' + \frac{3k_B T_c}{e} \right) J_c - \left(\phi' + \frac{3k_B T_h}{e} \right) J_h e^{-\frac{eV}{k_B T_h}} - \frac{T_h - T_c}{R}. \tag{3}$$

Here, $J_c = A^* T_c^3 \exp[-(e\phi')/k_B T_c]$ ¹³ is the thermionic current density emitted from the cold graphene electrode at temperature *T_c* over an effective Schottky barrier height of ϕ' formed at the interface between the vdW structure and the graphene electrode. Similarly, we have $J_h = A^* T_h^3 \exp[-(e\phi')/k_B T_h]$ for the thermionic current density emitted from the hot graphene electrode at temperature *T_h*. Due to the unique properties of graphene in tuning its Fermi energy via bias voltage or chemical doping, the effective barrier is defined as $\phi' = \phi - E_F/e$, where ϕ is the value at zero bias with an intrinsic Fermi level.

As already pointed out by previous work^{13,36}, traditional vacuum thermionic converter cannot operate near room temperature due to the high vacuum work function (around 4.51 eV) of graphene. To operate at room temperature, the work function is required to be below 0.34 eV³⁶, which can be attainable in the graphene/TMDs heterostructure. In Fig. 2, we present the verification (in comparison with experimental results) of the revised thermionic emission law¹³ is valid in describing the electron flow over the Schottky barrier of graphene/TMDs contact for graphene/MoSe₂ (44 layers) contact²⁴ with a reported barrier height of $\phi' = 0.2$ V (best fit). The calculated value of $\ln(J/T^3)$ has an excellent agreement with experiment²⁴ from $1000/T$ (about *T* = 250 to 300 K) as shown in Fig. 2a. The agreement with experiment indicates that our thermionic emission model can be good enough to describe the carrier's transport across the Vdw heterostructure.

A prior first-principles calculation³⁷ has also indicated that the conduction band edge of MoSe₂ will reduce with increasing layer number (black line with black symbols in Fig. 2b). As a result, the Schottky barrier height decreases from 0.614 to 0.38 volt as the layer number increases from one layer to eight layers (red line with symbols) as shown in Fig. 2b. The trend of change in Schottky barrier height with increasing layer number is consistent with previous experiment²⁴, which reports that the Schottky barrier height between graphene and MoSe₂ becomes saturable with larger than 50 MoSe₂ layers. Based on the experiment facts and first-principle calculation, it is reasonable to believe that the Schottky barrier height can be reduced down to around 0.2 volt when the layer number increases up to 44 layers. For completeness, the band structure of other contacts between graphene and one layer of TMDs materials (MoS₂, WS₂ and WSe₂) can be found in the Supplementary materials (see S3).

In Eq. (3), the $3k_B T$ term measures the average heat energy per emitted electron, which is obtained through the internal energy of electron in graphene associated with one degree of freedom, $U = k_B T^2 \left(\frac{d \ln(\Xi(k))}{dT} \right)$, with $\Xi(k)$ being the partition function. In the last term of Eq. (3), R is the thermal resistance including all the contributions due to interface (between graphene and TMDs, and different layers within TMDs), barrier layers and electrode. We will only consider thermal conductance due to TMDs and limit our study to multi-layers TMDs, as the molecular dynamics simulation (see discussions section) shows that the contribution from the interface between graphene and TMDs and electrode is small, as compared to the resistance due to TMDs itself. For simplicity and a conservative estimation, we use $R = d/\kappa$ in Eq. (3). Including other effects will increase the efficiency predicted in this paper. By defining the average temperature as $T = (T_h + T_c)/2$, and the temperature difference as $\delta T = T_h - T_c$, we calculate J_e as the thermionic emitted current density at the mean temperature T . In the limit of $\delta T \ll T$ and $eV \ll k_B T$, Eqs (2) and (3) become

$$J_e = J_G \left(\frac{eV}{k_B T} - (\alpha + 3) \frac{\delta T}{T} \right), \quad (4)$$

$$J_Q = J_G (\alpha + 3) \frac{k_B T}{e} \left(\frac{eV}{k_B T} - (\alpha + 3 + \beta) \frac{\delta T}{T} \right), \quad (5)$$

where $\alpha = e\phi'/k_B T$, $\beta = \frac{\gamma+3}{\alpha+3}$, $\gamma = (T_R/T)^3 e^\alpha$, and $(k_B T_R)^3 = \pi \hbar^3 v_f^2 / (k_B R)$. Here, we have introduced a temperature-like parameter T_R to characterize the performance of the device (together with the effective barrier height, ϕ'), where T_R is proportional to $(\kappa/d)^{1/3}$ or inversely proportional to the barrier resistance, $R^{-1/3}$. Numerically, we have $T_R [\text{K}] = 4666 \times (\kappa/d)^{1/3}$ for κ [W/m/K] and d [nm].

The experimental verification of our model proposed in this work closely depends on the design of Gr/TMDs/Gr. In this paragraph, we will briefly state that our design of Gr/TMDs/Gr can be easily realized by using the current capability in fabrication of vdW heterostructure by many different research groups^{22–24}. For example, Gr/WSe₂/Gr had been fabricated ranging from $d = 2.2$ nm (3 layers of WSe₂) to 40 nm²². Similarly, we have $d = 50$ nm and $d = 9$ to 50 nm, respectively, for Gr/MoS₂/Gr²³, and for Gr/MoSe₂/Gr²⁴. The combination of more than one type of TMDs materials is also possible, such as Gr/MoS₂/WSe₂/Gr³⁸. Thus we have used some of reported experimental parameters to illustrate the performance of our design in harvesting waste heat at 400 K as shown below.

Results

Refrigerator. For the device to operate as a refrigerator, it require $J_Q > 0$, which poses a condition of $\frac{eV}{\alpha+3+\beta} > k_B \delta T$ in Eq. (5). The cooling efficiency is calculated by $\eta = J_Q / (J_e \times V)$ and its maximum efficiency (η_{max}) is obtained by taking first derivative with respect to V , which gives

$$\frac{\eta_{max}}{T/\delta T} = \frac{\alpha + 3}{(\sqrt{\alpha + 3 + \beta} + \sqrt{\beta})^2}. \quad (6)$$

The variables α and β are functions of ϕ' and T_R . The term $T/\delta T$ is approximately regarded as the Carnot efficiency. In Fig. 3, we plot the maximum cooling efficiency η_{max} (in terms of the Carnot efficiency) at $T_c = 260$ K as a function of effective barrier height $\phi' = 0$ to 0.5 volt for various $T_R = 500$ K down to 10 K at $T_h = 300$ K (solid lines) and 350 K (dashed lines). It is clear that the cooling efficiency increases with smaller T_R as expected. For a given T_R , the maximal efficiency can be achieved by tuning the effective barrier height ϕ' . The tuning range will become wider for higher temperature (e.g. $T_h = 350$ K) as compared to $T_h = 300$ K. In the limit of $T_R = 0$, we have $\gamma = 0$, $\beta = \frac{2}{\alpha+3}$, and Eq. (6) becomes $\eta_{max}/(T/\delta T) = 1/(\sqrt{1 + 2/(\alpha + 3)^2} + \sqrt{2/(\alpha + 3)^2})^2$, which depends only on α (or ϕ').

With few reported values of the cross-plane thermal conductivity for vdW heterostructure, we use two measurements (at 300 K)^{27,39} to illustrate the realistic cooling efficiency of our design. For Gr/WSe₂/Gr with $d = 62$ nm and $\kappa = 0.048$ W/m/K, we have $T_R = 425$ K and our design predicts a cooling efficiency of 26.11% of the Carnot efficiency with an optimal barrier $\phi' \approx 0$ (Ohmic contact). For Gr/MoSe₂/Gr with $d = 70$ nm and $\kappa = 0.0847$ W/m/K, we have $T_R = 496$ K and the cooling efficiency is 21.94% of the Carnot efficiency with an ohmic contact too. If the T_R can be engineered to be less than 300 K, the maximum efficiency will occur at some optimal values of $\phi' = 0.05$ to 0.3 volt, which are also within the current tunable range for Gr/WSe₂ and Gr/MoSe₂ contacts^{24,40}.

For practical TE-based coolers used in various applications (e.g. air-conditioned car seats, and semiconductor laser cooling), the efficiency is less than 15% of the Carnot efficiency⁴¹. With the highest reported value of $ZT = 2.4$ for Bi₂Te₃/Sb₂Te₃ superlattice structure⁶, the efficiency will become 31.1% of the Carnot efficiency at the

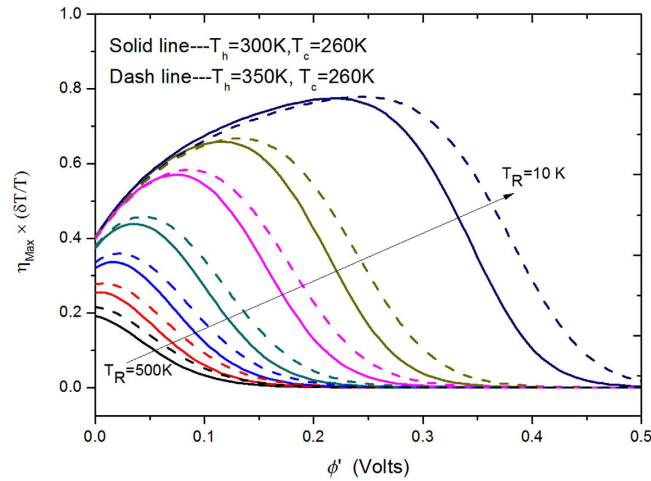


Figure 3. The maximum cooling efficiency η_{max} (in terms of the Carnot efficiency) as a function of barrier height ϕ' at $T_c = 260$ K for $T_h = 300$ K (solid lines) and 350 K (dashed lines) from T_R [K] = 500, 400, 300, 200, 100, 50 and 10 (according to the arrow direction).

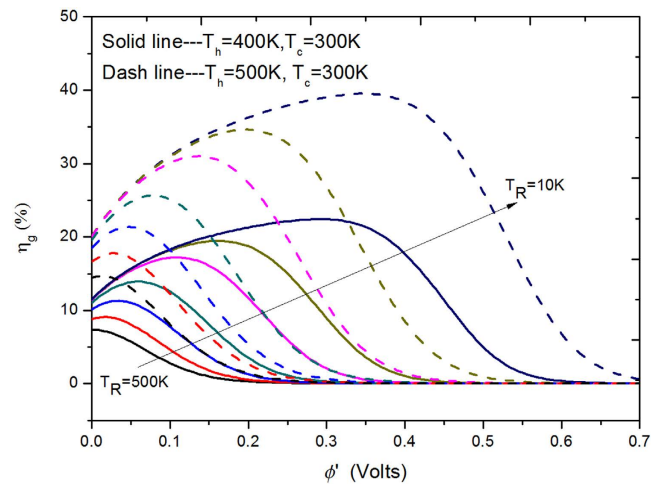


Figure 4. The power generation efficiency η_g as a function of barrier height ϕ' at $T_c = 300$ K for $T_h = 400$ K (solid lines) and 500 K (dashed lines) from T_R [K] = 500, 400, 300, 200, 100, 50 and 10 (according to the arrow direction).

same temperature studied here. For practical applications, the refrigerator has to pump a heat flux of a few hundreds W/cm^2 . For our design, the pumped heat current is estimated by $J_Q \approx 3A_G T_c^2 \phi' (T_h - T_c) \times \exp(-e\phi'/k_B T_c)$ where $A_G = 0.01158 \text{ A}/\text{cm}^2/\text{K}^3$. At $T_c = 260$ K, $T_h = 300$ K, and $\phi' = 0.05$ volt, the estimated cooling power is up to $500 \text{ W}/\text{cm}^2$, which is larger than those of thin-film Bi_2Te_3 -superlattice thermoelectric cooling devices⁴². At higher range of $T = 400$ to 500 K, our design will give about 1.7 to $3 \text{ kW}/\text{cm}^2$.

Power generator. When the current flow is from hot side to cold side (e.g. $T_h = 400$ K and $T_c = 300$ K), the device will behave as a power generator. This current flow via an external circuit is then extracted as the power output by harvesting the thermal energy from the heated graphene electrode (hot side). The maximal value of the power generation efficiency is calculated by

$$\eta_g = \delta T/T \times (\sqrt{\alpha + 3 + \beta} - \sqrt{\beta})^2 / (\alpha + 3). \quad (7)$$

The calculated results are plotted in Fig. 4 as a function of ϕ' for $T_R = 500$ K down to 10 K at a fixed $T_c = 300$ K for two heat sources: $T_h = 400$ K (solid lines) and 500 K (dashed lines). At $T_h = 400$ K, the efficiency is from about 8% to 20% for $T_R = 500$ K down to 10 K. Assuming $\kappa = 0.08 \text{ W}/\text{m}/\text{K}$ and $d = 89 \text{ nm}$, this corresponds to $T_R = 450$ K and η_g is about 8% (with $\phi' \approx 0$), which is comparable to or better than some of highly-efficient thermal harvesting devices, such as (a) a two-layer WSe_2 TE-based device ($ZT = 1.6$) having a maximum efficiency of 6.5% ⁹, (b) an electrochemical system for harvesting low-grade waste heat energy (<100 °C) with efficiency less than 8% ⁴³, and (c) a theoretical efficiency of 8% for $ZT = 2.4$ TE material at 400 K ¹. Note that the efficiency for a power generator

is very sensitive to heat source temperature. When T_h is increased from 400 K (solid lines) to 500 K (dash lines), the efficiency increases by a factor of about 2 as shown in Fig. 4.

Based on the available experimental data^{27,28,39}, we calculate (see Table 1) the efficiencies of harvesting heat at 400 K (cold side is kept at 300 K) for some practical design parameters: (a) Gr/MoSe₂/Gr with $d = 50$ nm, (b) Gr/WS₂/Gr with $d = 50$ nm, (c) Gr/MoSe₂/Gr with $d = 70$ nm, and (d) Gr/WSe₂/Gr with $d = 62$ nm. The table shows that the operating range of T_R is from 850 K down to 428 K, with efficiency from 3.15% to 8.56%. The efficiency for both Gr/MoSe₂/Gr and Gr/WSe₂/Gr is about 7% to 8%, which is better than 3% to 4% generated by Gr/MoSe₂/Gr and Gr/WS₂/Gr. Note that we only use $T_h = 400$ K as an example in the table. For other heat source temperatures T_h (with $T_c = 300$ K), the efficiency of the energy harvesting using these common vdW heterostructures can be estimated based on the fitted equation determining the cross-plane thermal conductivity as a function of temperature by $\kappa = a + bT + cT^2 + dT^3$, where a , b , c and d are the fitting parameters, and they can be found in the Supplementary materials (see S2).

Discussions

In our model, the tunneling of low-energy electrons through the Schottky barrier at the interface will become important if the width of the barrier is small³⁵. This consideration imposes a lower limit to the layer thickness d in our design to ensure that the injection of the electrons from the graphene electrode across the barrier is governed by the over-barrier process (thermionic emission) as assumed in the model. This minimal d may be estimated by using $d_{min} \approx \sqrt{e\phi^2/\hbar^2/8k_B^2 T^2 m^*}$, with m^* being the effective electron mass of the barrier layers⁴⁴, which gives $0.845m_e$, $0.776m_e$, $0.665m_e$, $0.643m_e$, respectively, for MoS₂, MoSe₂, WS₂ and WSe₂. For Gr/WS₂/Gr, it was reported that thermionic emission will be dominant for 5 layers or more³⁵. For Gr/WSe₂/Gr and Gr/MoSe₂/Gr, the minimal thickness is estimated to be, respectively 5 and 4 nm based on Simmons model⁴⁵.

For few-layer TMDs (MoS₂, MoSe₂, WS₂ and WSe₂), their cross-plane lattice thermal conductivity is very small compared to traditional TE materials, which is in the range of 0.01 to 0.1 W/m/K due to the localized lattice vibrations or the disorder within the TMDs^{27–29,39}. It was claimed that the reduction is also valid for other reassembled TMDs²⁷, and thus considering $d = 50$ nm and $\kappa = 0.01$ W/m/K, we have T_R around 272.6 K, which implies that it is positive to realize the calculated efficiencies of about 10% in harvesting waste heat at 400 K or 20% at 500 K as shown in Fig. 4 for $T_R = 300$ K.

As T_R scales as $(\kappa/d)^{1/3}$, to further reduce T_R down to 100 K or even 10 K, the lattice cross-plane thermal conductivity κ must be reduced for a fixed thickness d . Further reducing d will not help as it will also promote the unwanted tunneling effect mentioned above. Thus, we conclude that our design will require vdW structure with low cross-plane thermal conductivity and reasonable thickness to function as a high-efficiency solid state thermionic device. A recent work for WSe₂⁴⁶ may have presented such a solution in increasing spacing of the layers, and stacking disorder, and it is possible have a further reduction in the cross-plane lattice thermal conductivity without reducing d . Another method to reduce the cross-plane thermal conductivity is by using superlattice composed of WSe₂ and MoSe₂. We speculate that a precise control of superlattice period thickness will be able to lead to a much lower cross-plane thermal conductivity together with fine-engineering thermal boundary resistance between different layers. If such extremely low cross-plane thermal conductivity can be realized experimentally, it is possible to have very high efficiency energy harvesting as indicated in Fig. 4.

As mentioned before, the interface resistance between graphene and the TMDs has been neglected in our model. To justify this assumption, a Molecular dynamics simulation has been done. The simulation details can be found in the section of Method and Supplementary Materials (see S1). In Fig. 5a, multiple layers of MoSe₂ (or WSe₂) are sandwiched by few-layers graphene with three layers on top and three at the bottom. The temperature distribution along the cross-plane direction of the hybrid multilayer structure, with an imposed heat flux $J_Q = 0.5$ GW/m² on the top graphene layer, is demonstrated in Fig. 5b. Note that small temperature drops near the heat source and heat sink are mainly induced by the artificial temperature control. From Fig. 5b, we see large temperature reduction $\Delta T_1 = 30$ K and $\Delta T_2 = 34$ K occurring at the two interfaces between graphene and MoSe₂, respectively at the interface between layers 3 and 4, and also between layers 11 and 12. In comparison, the total temperature drop is about 2.8 K per layer for the eight layers of MoSe₂ (one order of magnitude lower). The thermal conductance (or Kapitza conductance) for these two interfaces is about $G = J/\Delta T = 16.56$ and 14.59 MW/m²/K, respectively. Note that the difference of G at the upper and the lower interface can be attributed to the temperature dependence of G ^{47,48}. These two values are larger than the cross-plane thermal conductance of a few-layer MoSe₂ by one to two orders of magnitude using the experiment data³⁹. Similar calculation has been repeated for WSe₂, which shows similar results (not shown). In Fig. 5c, we show that the interface thermal conductance for WSe₂ and MoSe₂ is almost independent of the numbers of layers, and the average value is about $G = 16.7$ MW/m²/K for Gr/MoSe₂/Gr and 17.12 MW/m²/K for Gr/WSe₂/Gr. Surprisingly, we find that our calculated interface conductance across graphene and MoSe₂ interface is very close to 25 MW/m²/K measured for graphene contact interface⁴⁸. From these findings, it is important to note that it is valid to consider the layer's resistance due to 2D TMDs in this paper as the first approximation. Subsequent improvement can be pursued through comparison with experimental verification (from other groups) on our calculated efficiency shown in Table 1 below. It is worth to mention that the calculated temperature gradient (around 50 K) across eight layers of MoSe₂ (or WSe₂) is consistent with the previous experiment³³. So it is reasonable to believe that more significant temperature gradient across more layers of MoSe₂ (or WSe₂) can be established. Compared with larger temperature drop across Gr/TMDs/Gr structure, the little temperature drop across Graphene layers can be ignored. In other words, the cross-plane thermal conductivity of graphene layers is much higher than that of TMDs. Therefore solid thermionic converter based on Gr/TMDs/Gr structure has better performance than pure graphene layers (Gr/Gr/Gr). In the Table 1, we study some well-known TMDs (MoS₂, MoSe₂, WS₂ and WSe₂) using the reported experimental parameters, it is found that MoSe₂ and WSe₂ are better candidates. They are able to harvest waste heat at 400 K with about 7% to 8% in efficiency. To further increase the efficiency of a power generator, the current model can

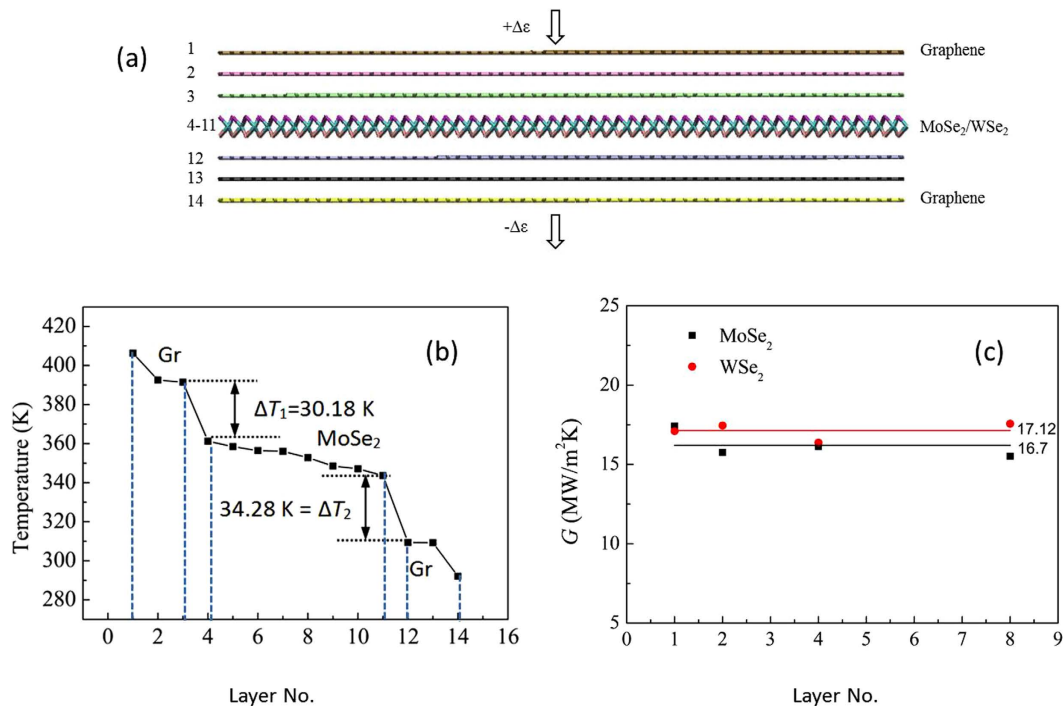


Figure 5. (a) Molecular dynamics model of interface thermal conductance of Gr/MoSe₂/Gr. (b) The temperature distribution across the Gr/MoSe₂/Gr vdW structure. Dotted lines are drawn to indicate the number of layers. (c) The interface thermal conductance (or Kapitza conductance) for Gr/MoSe₂/Gr and Gr/WSe₂/Gr as a function of the number of layers.

be also extended to include the contribution from solar energy and other thermal effects^{49–51}. As a refrigerator, the cooling efficiency is about 0.22 to 0.26 of the Carnot efficiency for a temperature difference of 40 K between 260 and 300 K. Note that the effects of finite electrical conductivity and thermal conductivity in the lateral direction on the proposed device's performance are not yet considered. The treatment of full model requires solving the coupling of Schrodinger and Dirac system, which is beyond the scope of this paper.

Similar to conventional TE devices, thermionic devices have lot of advantages, such as no moving parts, no noise, high reliability, long service time and so on. These features enables many possible applications for thermionic power generation and thermionic cooling. The most promising application for TIC is wasted heat recovery from vehicles to improve fuel economy. Other potential applications include harvesting industrial waste heat (e.g. steel rolling mill, cement, glass manufacture plant, etc.) and domestic heat (e.g. water heater). for electricity or charging batteries. While for thermionic cooling, most possible application is on-chip cooling of nanoelectronics devices. But the application can be extended to integrate with targeted devices to maintain the low-temperature environment for semiconductor laser, medical and scientific equipments. Finally, the vertical transport of charge transport at the graphene-semiconductor interface remains interesting. Modified Schottky models have been formulated to study the inhomogeneous of Schottky barrier at the interface⁵² and also the smooth transition between the T³ and T² temperature scaling⁵³.

Methods

The interlayer distances between the graphene and MoSe₂ (or WSe₂) are set to 3.35 Å which is interlayer distance of bulk graphite. The interlayer distance between the MoSe₂ (or WSe₂) layers is 3.11 Å (or 3.14 Å) according to previous first-principle calculation⁵⁴. The in-plane dimensions of the layer considered here are 69 Å × 70 Å. Periodic boundary conditions are applied along the in-plane directions and free boundary conditions are applied along the cross-plane direction of heterostructure. In the simulation, the initial configuration is equilibrated by using the constant volume and temperature (NVT) ensemble at a temperature T for 50 ps with a time step $\Delta t = 0.5$ fs. Upon realization of the equilibrium state, the system is switched to the constant volume and energy (NVE) ensemble to maintain the energy conservation condition. A constant heat flux is then imposed into the system at each time step by adding a small amount of heat $\Delta\varepsilon$ into the upmost graphene layer (layer 1). In doing so, we reduce the same amount of energy from the graphene layer at the bottom (layer 14). The simulation is conducted until a stable temperature gradient is established along the heat flux direction. For a hybrid system consisting of different interfaces, a temperature drop ΔT_{in} at the interface is usually developed, which gives a measurement of the interface thermal conductance or the Kapitza conductance $G = J/\Delta T_{in}$, where $J = \Delta\varepsilon/A\Delta t$ with A denoting the cross-section area.

References

- Vining, C. B. An inconvenient truth about thermoelectrics. *Nat. Mat.* **8**, 83–85 (2009).
- Kim, H. S., Liu, W., Chen, G., Chu, C.-W. & Ren, Z. Relationship between thermoelectric figure of merit and energy conversion efficiency. *PNAS* **112**, 8205–8210 (2015).
- Hicks, L. D. & Dresselhaus, M. S. Effect of quantum-well structures on the thermoelectric figure of merit. *Phys. Rev. B* **47**, 12727–12731 (1993).
- Dresselhaus, M. S. *et al.* New directions for low-dimensional thermoelectric materials. *Adv. Mater.* **19**, 1043–1053 (2007).
- Zebarjadi, M., Esfarjani, K., Dresselhaus, M., Ren, Z. & Chen, G. Perspectives on thermoelectrics: from fundamentals to device applications. *Energy and Environment Science* **5**, 5147–5162 (2012).
- Venkatasubramanian, R., Siivola, E., Colpitts, T. & Quinn, B. O. Thin-film thermoelectric device with high room-temperature figures of merit. *Nature* **413**, 597–602 (2001).
- Harman, T., Walsh, M., Laforge, B. & Turner, G. Nanostructured thermoelectric materials. *J. Electron. Mater.* **34**, L19–L22 (2005).
- Li, J.-F. *et al.* High-performance nanostructured thermoelectric materials. *NPG Asia Materials* **2**, 152–158 (2010).
- Hippalgaonkar, K. *et al.* Record high thermoelectric powerfactor in single and few-layer MoS₂. *Preprint at* <http://arxiv.org/abs/1505.06779> (2015).
- Wan, C. *et al.* Flexible n-type thermoelectric materials by organic intercalation of layered transition metal dichalcogenide TiS₂. *Nat. Mater.* **14**, 622–627 (2015).
- Huang, W. *et al.* Theoretical study of thermoelectric properties of few-layer MoS₂ and WSe₂. *Phys. Chem. Chem. Phys.* **16**, 10866–10874 (2014).
- Hatsopoulos, G. N. & Kaye, J. Measured thermal efficiencies of a diode configuration of a thermo electron engine. *J. Appl. Phys.* **29**, 1124 (1958).
- Liang, S.-J. & Ang, L. K. Electron thermionic emission from graphene and a thermionic energy converter. *Phys. Rev. Appl.* **3**, 014002–014010 (2015).
- Zhu, F. *et al.* Heating graphene to incandescence and the measurement of its work function by the thermionic emission method. *Nano Res.* **7**, 553–560 (2014).
- Geim, A. K. & Grigorieva, I. V. Van der waals heterostructures. *Nature* **499**, 419–425 (2013).
- Shakouri, A. & Bowers, J. E. Heterostructure integrated thermionic coolers. *Appl. Phys. Lett.* **71**, 1234–1236 (1997).
- Mahan, G. D. & Woods, L. M. Multilayer thermionic refrigeration. *Phys. Rev. Lett.* **80**, 4016–4019 (1998).
- Vashaee, D. & Shakouri, A. Improved thermoelectric power factor in metal-based superlattices. *Phys. Rev. Lett.* **92**, 106103–106107 (2004).
- ODwyer, M. F., Levis, R. A., Zhang, C. & Humphrey, T. E. Efficiency in nanostructured thermionic and thermoelectric devices. *Phys. Rev. B* **72**, 205330–205340 (2005).
- Vashaee, D. & Shakouri, A. Electronic and thermoelectric transport in semiconductor and metallic superlattices. *J. Appl. Phys.* **95**, 1233 (2004).
- Lin, Y. C. *et al.* Atomically thin resonant tunnel diodes built from synthetic van der waals heterostructures. *Nat. Commun.* **6**, 7311 (2015).
- Massicotte, M. *et al.* Picosecond photoresponse in van der waals heterostructures. *Nat. Nanotechnol.*, doi: 10.1038/NNANO.2015.227 (2015).
- Yu, W. J. *et al.* Highly efficient gate-tunable photocurrent generation in vertical heterostructures of layered materials. *Nat. Nanotechnol.* **8**, 852–858 (2013).
- Sata, Y. *et al.* Electric field modulation of schottky barrier height in graphene/MoSe₂ van der waals heterointerface. *Appl. Phys. Lett.* **107**, 023109 (2015).
- Cao, X., Tan, C., Zhang, X., Zhao, W. & Zhang, H. Solution-processed two-dimensional metal dichalcogenide-based nanomaterials for energy storage and conversion. *Advanced Materials* **28**, 6167 (2016).
- Zhang, H. Ultrathin two-dimensional nanomaterials. *ACS Nano* **9**, 9451 (2015).
- Chiritescu, C. *et al.* Ultralow thermal conductivity in disordered layered WSe₂ crystals. *Science* **315**, 351–353 (2007).
- Muratore, C. *et al.* Cross-plane thermal properties of transition metal dichalcogenides. *Appl. Phys. Lett.* **102**, 081604–081608 (2013).
- Paul, B. *et al.* Large-area synthesis of WSe₂ from WO₃ by selenium-oxygen ion exchange. *2D Mater.* **2**, 014003–014010 (2015).
- Kim, J.-Y., Choi, S. M., Seo, W.-S. & Cho, W.-S. Thermal and electronic properties of exfoliated metal chalcogenides. *Bull. Korean Chem. Soc.* **31**, 3225–3227 (2010).
- Humphrey, T. E., ODwyer, M. F., Zhang, C. & Levis, R. A. Efficiency in nanostructured thermionic and thermoelectric devices. *J. Appl. Phys.* **98**, 026108 (2005).
- Kima, R., Jeong, C. & Lundstrom, M. S. On momentum conservation and thermionic emission cooling. *J. Appl. Phys.* **107**, 054502 (2010).
- Chen, C.-C., Li, Z., Shi, L. & Cronin, S. B. Thermoelectric transport across graphene/hexagonal boron nitride/graphene heterostructures. *Nano Res.* **8**, 666–672 (2015).
- Wang, X., Zebarjadi, M. & Esfarjani, K. First principlwanges calculations of solid-state thermionic transport in layered van der waals heterostructures. *Nanoscale* **8**, 14695 (2016).
- Georgiou, T. *et al.* Vertical field effect transistor based on graphene-WS₂ heterostructures for flexible and transparent electronics. *Nat. Nanotechnol.* **8**, 100–103 (2012).
- Mahan, G. D. Thermionic refrigeration. *J. Appl. Phys.* **76**, 4362–4366 (1994).
- Kang, J., Tongay, S., Zhou, J., Li, J. & Wu, J. Band offsets and heterostructures of two-dimensional semiconductors. *Appl. Phys. Lett.* **102**, 012111–012115 (2013).
- Lee, C.-H. *et al.* Atomically thin p-n junctions with van der waals heterointerfaces. *Nat. Nanotechnol.* **9**, 676–681 (2014).
- Chiritescu, C. Ultralow thermal conductivity in layered disordered crystalline materials. *Ph.D Thesis, University of Illinois at Urbana-Champaign* (2010).
- Chuang, H.-H. *et al.* High mobility WSe₂ p- and n-type field effect transistors contacted by highly doped graphene for low-resistance contacts. *Nano. Lett.* **14**, 3594–3061 (2014).
- Brown, D., Fernandez, N., Dirks, J. A. & Stout, T. B. *The Prospects of Alternatives to Vapor Compression Technology for Space Cooling and Food Refrigeration Applications* (Pacific Northwest National Laboratory (PNL). U.S. Department of Energy, March 2010).
- Bulman, G. E., Siivola, E., Shen, B. & Venkatasubramanian, R. Large external δt and cooling power densities in thin-film Bi₂Te₃-superlattice thermoelectric cooling devices. *Appl. Phys. Lett.* **89**, 122117–122120 (2006).
- Lee, S. W. *et al.* An electrochemical system for efficiently harvesting low-grade heat energy. *Nat. Commun.* **5**, 3942–3948 (2014).
- Darshana Wickramaratne, F. Z. & Lake, R. K. Electronics and thermoelectric properties of few-layer transition metal dichalcogenides. *J. Chem. Phys.* **140**, 124710–124723 (2014).
- Simmons, J. G. Generalized formula for the electric tunnel effect between similar electrodes separated by a thin insulating film. *J. Appl. Phys.* **34**, 1796–1803 (1963).
- Erhart, P., PerHyldgaard & Lindroth, D. O. Microscopic origin of thermal conductivity reduction in disordered van der waals solids. *Chem. Mater.* **27**, 5511–5518 (2015).
- Liu, B. *et al.* Interfacial thermal conductance of a silicene/graphene bilayer heterostructure and the effect of hydrogenation. *ACS Appl. Mat. Interfaces* **6**, 18180–18188 (2014).

48. Koh, Y. K., Bae, M.-H., Cahill, D. G. & Pop, E. Heat conduction across monolayer and few-layer graphenes. *Nano. Lett.* **10**, 4363–4368 (2010).
49. Segev, G., Rosenwaks, Y. & Kribus, A. Efficiency of photon enhanced thermionic emission solar converters. *Sol. Energ. Mat. Sol. Cells* **107**, 125–130 (2012).
50. Schwede, J. W. *et al.* Photon-enhanced thermionic emission for solar concentrator systems. *Nat. Mater.* **9**, 762–767 (2010).
51. Li, X. *et al.* Graphene-on-silicon schottky junction solar cells. *Advanced Materials* **22**, 2743 (2010).
52. Liang, S. J. *et al.* A modified Schottky model for graphene-semiconductor (3D/2D) contact: A combined theoretical and experimental study. *IEEE International Electron Device Meeting (IEDM)*, 14.4.1–14.4.4 (2016).
53. Ang, Y. S. & Ang, L. K. Current-temperature scaling for a Schottky interface with non-parabolic energy Dispersion. *Phys. Rev. Appl.* **6**, 034013 (2016).
54. Yun, W. S. *et al.* Thickness and strain effects on electronic structures of transition metal dichalcogenides: 2h-m x 2 semiconductors (m = mo, w; x = s, se, te). *Phys. Rev. B* **85**, 033305 (2012).

Acknowledgements

This work was supported by SUTD-MIT IDC Grant (IDG21200106 and IDD21200103) and Singapore MOE T2 Grant (T2MOE1401). L. K. Ang acknowledges the support of AFOAR AOARD grant (FA2386-14-1-4020).

Author Contributions

S.J.L. conceived the project, B.L. and K.Z. performed the molecular dynamics simulation, W.H. did the first-principle calculations. S.J.L. and L.K.A. wrote the manuscript with contributions from the other authors.

Additional Information

Supplementary information accompanies this paper at <http://www.nature.com/srep>

Competing Interests: The authors declare no competing financial interests.

How to cite this article: Liang, S.-J. *et al.* Thermionic Energy Conversion Based on Graphene van der Waals Heterostructures. *Sci. Rep.* **7**, 46211; doi: 10.1038/srep46211 (2017).

Publisher's note: Springer Nature remains neutral with regard to jurisdictional claims in published maps and institutional affiliations.



This work is licensed under a Creative Commons Attribution 4.0 International License. The images or other third party material in this article are included in the article's Creative Commons license, unless indicated otherwise in the credit line; if the material is not included under the Creative Commons license, users will need to obtain permission from the license holder to reproduce the material. To view a copy of this license, visit <http://creativecommons.org/licenses/by/4.0/>

© The Author(s) 2017